In situ stress measurements interpretations in large underground marble quarry by 3D modeling

UNIVERSITÀ DEGLI STUDI DI TORINO

errero. A.M, Migliazza M.R, Segalini A., Gullì (2013) In situ stress measurements interpretations in large underground marble quarry by 3D modeling International journal of rock mechanics Volume 60, June 2013, 103-113

doi: 10.1016/j.ijrmms.2012.12.008

In situ stress evaluation near faults through DEM modelling

Abstract

The design of underground voids of significant size and of a complex geometry is often accompanied by the use of numerical models that are able to estimate the range of stress and strain induced by the excavations and consequently to evaluate the stability conditions of the voids. In this context, it is essential to define the natural state of stress of the rock mass, the mechanical properties of the rock matrix and the discontinuities and to carry out some in situ measurements to calibrate the final model.

In the Carrara basin (Italy) there is a huge number of underground excavations that need to be monitored and, for this purpose, a series of models and in situ measurements have been performed. This work was conducted to point out the difficulties involved in the understanding of the on site measured stress. A series of tests was conducted by the technical staff of the Working Environment Safety Office (USL) in Carrara, in the quarry called "Faniello", due to complex tectonic environment in the area.

A series of comparisons between 3D DEM numerical models has been performed in order to understand the influence of the presence of the main faults on the in situ state of stress.

Introduction

The knowledge of in situ stress on the earth's crust is important in many rock engineering problems. Stresses in rocks can only be measured in certain points, and the in situ determination of the stress state in large rock masses involves many assumptions and is influenced by various factors, one of the most important being the presence of discontinuities. A discontinuity can have a relevant influence on the magnitude and orientation of the stress components in the rock. The results of in situ measurements indicate that a re-orientation and variation in magnitude of the stresses occur close to the discontinuities and that there are jumps in stress (or stress discontinuity) on one side or other of the discontinuity.

The role of discontinuities is the most relevant topic, in most of instability phenomena, but, as pointed out by Diederichs (1999), the stresses in the rock mass may play - and in some of the recorded accidents, have played - a relevant role, and the estimation of the stress state in the rock masses in which these shallow ornamental rock mines are located is therefore a topic of paramount interest.

Understanding and estimating the stress state of a rock became increasingly relevant over the last quarter of the last century as numerical models became one of the most popular rock engineering design tools (Segalini et al., 2009, Alejano et al., 1999, Alejano et al., 2008), and it has not always easy to have precise values available for the components of the in situ rock stress state. (Hudson & Cornet, 2003). Moreover, several studies have shown that the stress field may present high local variation and

scattered patterns in jointed rock masses (Hudson, 2010). Although stress estimation methods can, in general, be considered reliable, it is still an extremely difficult task to try to make an overall interpretation of individual and combined measurements, and of the local and general in situ stress states, as well as their comparison with numerical modelling predictions (Hudson & Cornet, 2003). As stated above, this is one of the main aims of the study here presented.

Numerical models appear useful to plan stress estimation campaigns as well as to interpret measurements. Numerical models should include as much as possible of the significant geological structure that may affect the rock mass stress distribution. Faults are particularly relevant, since they can cause a significant variation in the stress distribution inside a rock mass.

It is therefore necessary, when carrying out numerical modelling, to strike a balance between over simplification and model complexity, a task that required considerable judgment. A well-prepared model can help in the design of field measurements by suggesting optimal locations for the tests. A numerical model can also assist in the interpretation of stress observations (Fairhurst, 2003).

Although a stress estimation campaign can usually provide information of great value for a particular project, it is important to be aware of how this information is used. The main aim of stress estimation should be to gain an understanding of the state of stress, and its variability, over a region. One or two measurements at specific locations may not be enough to allow extrapolation to a larger region. In mountainous areas, topographic effect may produce considerable local variability in the stresses. (Fairhurst, 2003)

In order to determine the effect of the presence of a single discontinuity and of its strength characteristics on the variation of the induced stress field, in terms of both magnitude and orientation of the main stresses, S. Su and O. Stephansson, 1999, conducted a numerical modelling using the Distinct Element Method in a bi-dimensional field (UDEC, Itasca). The modelling involves using a model made up of two blocks separated by a discontinuity and subject to a bilateral stress state acting on the boundary; the blocks have linear elastic behaviour and the discontinuity has a stress that is expressed through the Mohr-Coulomb criterion.

As expected, the orientation of the main stresses close to the discontinuity is parallel and perpendicular to the discontinuity itself, but far from the discontinuity, it progressively turns until it reaches the direction of the main stresses at the boundary. The parametric analyses have made it possible to conclude that the re-orientation range of the stresses is determined to a great extent by the friction angle (φ) of the discontinuity, and, to a lesser extent, by the lateral confinement coefficient (k_o) and the angle between the discontinuity and the direction of the maximum main stress applied at the boundary (σ). The orientation range diminishes as the friction angle increases.

In order to go over and complete the study conducted by Su in a 3D field, an analogous distinct element numerical modelling has been conducted (3DEC, Itasca) in which the tri-dimensional computational model is a cube (Figure 1) made up of two blocks separated by a discontinuity and subjected to a normal stress field applied at the boundary; like the previous model, the blocks have been assumed to have linear elastic behaviour and the discontinuity to have strength that is expressed through the Mohr-Coulomb criterion, while the cohesive contribution has been considered nil. A series of parametric analyses was then conducted varying the stress state applied at the boundary (and the friction angle of the discontinuity) and, in particular, the lateral stress coefficient k_o (considered constant in the two directions x and y) was considered to vary between 1 and 2.5, while the friction angle – was varied between 0 and 35°.

Figure 1 – Geometry of the 3D DEM model and its loading condition (a); vertical section considered for the comparison of the results (b).

In all the analyses that were carried out, it was possible to observe that, along a vertical section that passed through the centre of the model (Figure 2), the orientation of the main stresses close to the marginal zones are equivalent to those of the stresses applied at the boundary. However, it was also observed that the main stresses progressively turn, in correspondence to the central zone, which is influenced by the presence of the discontinuity, until they are arranged parallel and perpendicular to the discontinuity itself.

Figure 2 – Main stresses in the central section parallel to the axis with a friction angle equal to 5°.

The influence of the stress state applied at the boundary was evaluated considering lateral thrust coefficient values of 1, 1.25, 1.67 and 2.5, and attributing a friction angle of 3° to the discontinuity and considering nil cohesion. The results were compared by analysing the trend of the maximum main stresses – (Figure 3) and the tangential stresses – (Figure 4) along a alignment perpendicular to the discontinuity and passing through the central point of the moment (alignment d in Figure 1). It is possible to note that the difference in the main stresses $\Delta\sigma$, in the zone around the discontinuity, increase with an increase in the lateral stress coefficient k_o, as do the tangential stresses --.

Figure 3 – Maximum main compression stresses

Figure 4– Shear stresses along the discontinuity

The influence of the strength characteristics of the discontinuity has been analysed considering a stress state at the boundary with a k_o value equal to 1.25 and a variable friction angle of the discontinuity. The

effect of this parameter can be observed in Figure 5, which shows the difference in value of the maximum main stresses calculated along the alignment in two points on either side of the discontinuity. It is possible to observe that, in the examined conditions, the maximum difference in the maximum main stresses occur for 0°, while the difference settles at a constant value for friction angles above 15°.

Figure 5- Differences in the main stresses in correspondence to the discontinuity in function of the friction angle – (K_o = 1.25)

The same model has been used to analyse the effect of the presence of the discontinuity on the border of an underground void (Figure 6). Again in this case, the same previously illustrated parametric analyses have been conducted (variation in the stress state at the border and variations in the friction angle), and the results show the re-orientation of the stresses near the discontinuity (Figure 7). As foreseeable, the excavation caused an increase in the stresses compared to the case without underground voids: in particular, a great concentration of stresses was observed at the edges of the tunnel.

Figure 6– Configuration of the model and the reference system

Figure 7– Main stresses in the central section parallel to the z axis

The variations in the components of the main stresses were calculated compared to the case without discontinuities in order to consider the effect of the mechanical characteristics of the discontinuity along the previously considered alignment d. The maximum variation in each main stress component is shown in Figure 8 for variations of the strength angle attributed to the discontinuity.

Figure 8- Differences in the maximum main stresses in correspondence to the discontinuity in function of the friction angle F (K_o = 1.25)

The reported modellings have made it possible to conclude that the re-orientation range of the stresses is influenced to a great extent by the friction angle φ of the discontinuity and, in particular, that it decreases with an increase in the friction angle and a decrease in k_o.

The importance of the reported considerations has shown that the interpretation of the stress states measured close to important discontinuities should be taken into account by means of discontinuity approaches that are able to simulate the rotation of the stresses in correspondence to the weakness plains.

In what follows we present an interpretation, based on 3D numerical modelling, of stress measurements performed in the vicinity of an underground excavation in the Carrara marble basin (Italy). The overcoring measurement method was used. This method is based on the principle of overcoring a pilot hole in which the soft inclusion measuring cell is installed. The principle of a soft cell is based on the theory of linear elasticity for continuous, homogenous and isotropic rocks (Sjöberg et al., 2003). The complete stress tensor at the test location can be determined by measuring six strain components in different directions on the wall of a borehole. The CSIRO hollow inclusion (HI) triaxial strain cell is used, which, in principle, allows the complete determination of the stress tensor from a single overcoring operation in one borehole (Ljunggren, 2003).

The quarry is characterised by the presence of three main faults that influence the state of stress; to a great extents for this reason, the study has been dedicated to studying the influence of the discontinuities on the state of stress through 3D DEM modelling, which is able to take into account the geometrical features of the rock mass and rock excavation.

Experimental site description

The exploitation area belongs to the metamorphic Apuan Alps complex and is the result of tectonic and metamorphic phases that occurred during the Alpine orogenesis. The current structure of the Apuan Alps is probably the result of a sharp rise, due to an isostatic response to the doubling of the continental crust that occurred in the past, and the consequent erosion of the Tuscan and Ligurian coatings, which created the tectonic window that allowed the Apuan Alps to emerge. The Apuan Alps is a metamorphic complex that originated after a low-grade metamorphism process (green schist facies) under a pressure of about 3-4 kbar and a temperature between 300° and 400° celsius. Under these conditions, limestone takes on a significant plasticity, and calcite crystals become larger, due to the temperature rise, and flatter to offer greater resistance to pressure. The subsequent placement of the rocks is a result of tectonic lifting of the earth's crust.

The quarry that has been studied, named "Faniello", is located in the Apuane Alps. The quarry is situated at the end of a valley in the Municipality of Stazzema (MS) at an altitude of 1190 m and it has a very steep topographic surface which, above the excavations, varies from 1200 m to 1430 m a.s.l.

A map of the excavations is shown in Figure 9, with indications of the stress state measurement points and of the main faults, which have resulted to be almost parallel and to have sub-vertical dips (of 86-88°) and dip directions of 150-160°.

Figure 9– Quarry excavation maps with indication of the in situ stress measurement points

The mechanical features of the rock material and of the rock joints (Table 1) were obtained from laboratory tests (uniaxial compressive tests, shear test and Brazilian tests) on the intact rock and on the discontinuities (shear tests) conducted on samples gathered in Carrara basin (Ferrero et al., 2003, Migliazza et al., 2011).

Table 1. mechanical parameters of intact rock and rock joints: E = Young's modulus; ν = Poisson's ratio; c_{ir} = intact rock cohesion ϕ_{ir} = intact rock friction angle; JKN = normal joint stiffness; JKS = shear joint stiffness; JRC = joint roughness coefficient; ϕ_j = joint friction angle; c_j = joint cohesion.

	Intact rock features
E (GPa)	40.3
ν (-)	0.182
c_{ir} (MPa)	21.4
ϕ_{ir} (°)	42
	Rock joint features
JKN (GPa/m)	40.3
JKS (GPa/m)	17.0
JRC (-)	12.6
ϕ_i (°)	32.3

The portion of the rock mass that has been investigated is located on the east side of the quarry and has an height of 5 m at the excavation face. The on site campaign began with stress measurements which were made through over-coring tests carried out using CSIRO cells, which allows 3D measurements to be made of the actual state of stress at the investigated position. The measurements were concentrated in the rock mass portion that characterizes the central room of the quarry. These measurements were conducted at a height of 1.8 m from the quarry floor.

Table 2 gives a detailed description of the positions of the conducted measurements obtained in terms of values and orientation of the main stress components (obtained by applying an elastic solution proposed by Sjoberg et al., 2003), while a stereographic projection of the main directions of the measured stresses is shown in Figure 10.

Table 2 main stress component for borehole 1 and 2

Borehole	Test	Distance from excavation wall [m]	Borehole dip [°]	σ_1 [MPa]	dip [°]	bear [°]	σ_2 [MPa]	dip [°]	bear [°]	σ_3 [MPa]	dip [°]	bear [°]
BH1	3D1_01	1,24	-3, 0	29,97	12	150	15,92	25	245	11,44	62	37
	3D1_02	2,65	-3, 0	28,86	45	148	13,97	7	246	9,91	44	342
	3D1_03	4,65	-3, 0	36,00	39	140	17,20	26	253	13,60	40	7
	3D1_04	8,60	-3, 0	30,00	35	155	12,33	3	64	7,60	54	330
	3D1_05	11,10	-4, 1	26,80	15	148	7,40	17	243	5,50	67	328
BH2	3D2_02	4,55	-4, 1	13,10	10	140	5,44	71	261	1,60	16	47

Figure 10- Representation of the network of action of the main stresses for the D1 tests (on the left) and D2 tests (on the right).

The mean orientation of the main in situ stresses was obtained through the use of the Dips programme (Rockscience Inc.) and the following result was obtained:

Table 3 – Mean orientation of the main stresses obtained during the D1 borehole test.

	Trend [°]	Plunge [°]
σ_1	147	29
σ_2	247	19
σ_3	352	56

It is important to observe that the main stresses are not perfectly vertical or horizontal and, above all, that the maximum component (σ_1) is not the vertical one. The measured stress state is surely influenced by the presence of the excavations, even in the most distant measurement point from the excavation wall which is located at a distance (11.5 m) that is no greater than twice the characteristic dimension of the excavation (about 5 m). Considering these values as the most representative of the pre-existing stress state of the quarry, a lateral confinement coefficient K_o, equal to the ratio between the horizontal stress – and the vertical stress –in the two horizontal directions x and z, was estimated, as a first approximation:

A fault, which represents the discontinuities that affect the examined rock mass, with a dip of 87° and a dip direction of 160°, has also been represented in the stereogram reported in Figure 10. In this way, it is possible to observe that the line of action of the maximum main stresses--, which we know to be of a compressive type, is perpendicular to the fault. This means that the examined rock mass can be presumed to be subject to a compression force perpendicular to the discontinuity plains, which tends to close the discontinuities themselves. --, the mean main stress, instead acts parallel to the discontinuities, while --, which is perpendicular to the two previous ones, is the vertical stress.

The stress measurement vs. depth are reported in Figure 10, where they are compared with the Kirsh elastic solution, considering an excavation depth that is varied between 240m (maximum depth) and 125 m (average depth), an excavation size of 5m and a unit weight of 27000 N/m^3.

Figure 11 – Comparison between the main in situ measured stress components and theoretical values calculated in an elastic field for a circular tunnel subject to an anisotropic stress state at different depths.

The conducted measurements are much higher than the values that could be estimated with elastic solutions, even under the hypothesis of maximum overburden (249 m), thus confirming the hypothesis of the presence of tectonic type strains.

Moreover, it is necessary to consider that, in this case, it is the minimum vertical stress that is vertical, while the mean and maximum ones are sub-horizontal and determined by a value of k_o equal to 4 and 1.4, respectively, in the different perpendicular horizontal directions (x and y respectively).

$$k_{0X}=\frac{\sigma_H}{\sigma_V}=\frac{\sigma_1}{\sigma_3}=\frac{26{,}80}{5{,}50}=4{,}87$$

$$k_{0Z}=\frac{\sigma_H}{\sigma_V}=\frac{\sigma_2}{\sigma_3}=\frac{7{,}40}{5{,}50}=1{,}35$$

The measurement of the existing stress state, the complexity and the articulated geometry of the excavations, and also the geostructural characteristics of the analysed rock mass, with particular reference to the three main faults that were identified, show that it is not possible to analyse this situation using 2D models or through modellings that consider the medium as a continuous equivalent and that it is instead necessary to resort to a 3D discontinuous model.

Analyses of the stress state of the Faniello quarry with DEM modelling

The numerical modelling concerned the analyses of the portion of the rock mass shown in Figure 12a, and it was conducted, considering the mass as a discontinuous medium, utilising the 3DEC (Itasca) calculation code.

The geometric model (Figure 12b), which has overall dimensions of 150 x 75 x 150 m, represents the area surrounding the portion of excavation along which the in situ measurements were conducted. The mass has three discontinuity plains which represent the main faults that are encountered in situ.

The model was elaborated considering that the blocks were deformable and that they had a linear elastic isotropic behaviour; the discontinuities are regulated by an elastic-plastic type of behaviour that considers collapse being reached according to the Mohr-Coulomb criterion. The adopted values of the physical-mechanical parameters, of the rocky matrix and of the joints are reported in Table 1.

Figure 12– Analysed portion of the excavation chamber and its simplification (a); geometric model utilised (b)

The geometric model was then subjected to a series of parametrical analyses which were conducted simulating different initial stress conditions in order to determine the best agreement with the in situ measured stress state.

The examined zone is in fact characterised by an elevated altimetric excursion of the topographic surfaces (varying from about 1430m to 1200 m a.s.l.); a vertical stress state was therefore imposed in the model which took into consideration the remarkable altimetric variation that characterises the rock mass (Figure 13– Geometry of the loads).

The conducted parametric analyses are summarised in Table 4: both constant and variable lithostatic stresses were considered along the extension of the model; isotropic and anisotropic stress conditions

along the horizontal plain with different lateral thrust coefficients; initial stress conditions above the lithostatic ones.

Figure 13– Geometry of the loads

Table 4. Parametrical analyses.

Model	1	2	3	4	5	6	7	8
Lythostatic stress	Yes	Yes	no	no	no	no	no	no
zγ	75γ	75γ	160γ	160γ	160γ	350γ	350γ	400γ
Horizzontal stress	isotropic	anisotropic	anisotropic	anisotropic	anisotropic	isotropic	anisotropic	anisotropic
k_{ox}	1	4	4	4	4	1	2	2
k_{oy}	1	1	1	1	1.4	1	1	1.5
Slope geometry	yes	Yes	yes	no	yes	yes	yes	yes
σ_{xx}	5.28	21.14	30.35	30.35	30.35	12.74	25.47	28.18
σ_{yy}	5.28	5.28	7.59	7.59	7.59	12.74	12.74	14.09
σ_{zz}	5.28	5.28	7.59	7.59	10.62	12.74	12.74	21.14

As expected, it was observed, in all the conducted modellings, that the presence of the discontinuities (Figure 14) induced a rotation of the main stresses in the zone in which the measurements were conducted.

Figure 14– Transversal and longitudinal sections of the model with respect to the excavation axis and representation of the main stress components.

The results obtained with the modelling were compared from the stress point of view, and the main stress components (σ_1) along an alignment of points created in the same position and direction in which the in situ tests had been conducted were analysed in particular.

A comparison between the values of the main stress components obtained from the numerical modelling with 3DEC and those obtained from the in situ measurements under a lithostatic hypothesis (Model 1) in both measurement positions is reported in Figure 15 and Figure 16, while the orientations of the main directions are compared in a similar manner in Table 5.

Figure 15 – Comparison of the in situ measured and D1 numerical modelling stresses.

Figure 16 – Comparison of the in situ measured and D2 numerical modelling stresses.

Table 5– Comparison of the mean datum obtained from the D1 numerical modelling and that obtained from the in situ measurements

	BH1				BH2			
	On site measure		3D model		On site measure		3D model	
	Trend	Plunge	Trend	Plunge	Trend	Plunge	Trend	Plunge
σ_1	147	29	179	36	140	10	173	13
σ_2	247	19	255	85	261	71	317	71
σ_3	352	56	1	37	47	16	79	10

A discrepancy can immediately be seen between the in situ measurements and the modelling results concerning both the values and the trend of the values with depth. In the illustrated case, the modelling has in particular underestimated all three of the stress components measured in the rock mass.

The complexity of the stress state that characterises the rock mass and the articulated geometrical conditions of the excavations make the calibration of the model rather complicated and it was considered necessary to conduct a back analysis procedure through the parametric analyses summarised in Table 4.

In order to establish which of the conducted modellings was closest to the real in situ situation, it proved necessary to conduct an overall evaluation process that took into consideration that some simulations gave a better approximation of the entity of some stress components while others were better at interpreting the orientation of the action line of the main stresses.

The global reliability of each model was then evaluated through the calculation of an "*equivalent percentage error*" that took into consideration the mean percentage error in the evaluation of the intensity of each main stress component ($\Delta\sigma$) and in the estimation of the angular orientation of the main directions ($\Delta\varphi$).

Therefore, the values and directions of the main stresses were calculated for each of the conducted analyses as well as in the corresponding measurement positions, and the differences with respect to the respective measurements were calculated, both in terms of value:

$$\Delta\sigma = \sigma_{mis} - \sigma_{cal}$$

and in orientation terms

$$\Delta\varphi = \varphi_{mis} - \varphi_{cal}$$

where φ is the acute angle between the line of action of the main stresses of the in situ measurements and of the modelling measurements.

The values of the equivalent errors were then calculated considering the three stress components at the same time:

$$\Delta\sigma = \Delta\sigma_1 + \Delta\sigma_2 + \Delta\sigma_3$$

$$\Delta\varphi = \Delta\varphi_1 + \Delta\varphi_2 + \Delta\varphi_3$$

The equivalent percentage error was determined by normalising the values with respect to the maximum value

$$\Delta\sigma_p = \frac{\Delta\sigma}{\max \Delta\sigma} 100$$

$$\Delta\varphi_p = \frac{\Delta\varphi}{\max \Delta\varphi} 100$$

In this way, it was possible to find the percentage errors made in the different modellings (Figure 17), and the effects were also summed.

Figure 17- Equivalent percentage errors calculated for each analysed model.

Simulation number 5 is the one that best minimizes the modelling error regarding a non lithostatic condition, non symmetrical confining state of stress and a realistic stress due to the slope topography. A comparison between the measured and computed stresses is shown in Figure 18.

Figure 18. Comparison between the measured and computed stresses in the borehole 5

Conclusions

A good correspondence between the in situ measured stress state and that calculated with a numerical code can only be obtained by imposing boundary conditions that are difficult to hypothesise for the stress state in a previous calibration phase.

In fact, it can be observed that in the examined case, the application of a lithostatic load led to an underestimation of the measured vertical stress state. It is also important to underline that, in this case, the vertical stress resulted to be the minimum main stress. The maximum main stress instead seemed to be a horizontal compression force perpendicular to the discontinuity systems which, in all probability, was due to the residual stresses derived from the orogenetic process of the Apuan Alps. The metamorphic Apuan complex is in fact the result of tectonic phases that occurred during the alpine orogenesis.

The difference between the in situ measurements and the modellings could be due to the fact that different factors are involved in rendering the determination of the stress state complicated, factors such as the presence of the tectonic forces that are still underway, which makes a stress due to a simple lithostatic load implausible.

Bibliography

Alejano L. García-Bastante, F., Alonso, E. y Taboada, J. (1999). Back Analysis of a Rock-burst in a shallow Gypsum Room & Pillar Exploitation. Proceedings of the 9th ISRM Congress. Paris. Ed. A.A. Balkema. Vol. I. pp. 1077-1080

Alejano, L.R., Taboada, J., Bastante, F.G., Rodríguez, P . (2008). Multi-approach back-analysis of a roof collapse in a mining room excavated in stratified rock. International Journal of Rock Mechanics and Mining Sciences. 45 (2008) 899-913.

Diederichs, M.D. (1999).Instability of Hard Rock masses: The Role of Tensile Damage and Relaxation. PhD Thesis, University of Waterloo, Ontario, Canada.

Amadei B. e Stephansson O. (1997) - *"Rock Stress and its Measurement"* - Chaman & Hall, London and New York;

A.M. Ferrero, A. Godio, L. Sambuelli, I. H. Voyat (2007) Geophysical and geo mechanical investigations applied to the rock mass characterization for distinct element modeling. Rock Mechanics and Rock Engineering. Springer Wien New York, Volume 40 (6), pp. 603-622. DOI 10.1007/s00603-006-0092-9.

Faihurst, Ch. (2003). Stress estimation in rock: a brief history and review. International Journal of Rock Mechanics & Mining Sciences. 40 (2003) 957-973.

Husdon, J.A. & Cornet, F.H. (2003). Preface Special Issue on rock stress estimation. International Journal of Rock Mechanics & Mining Sciences. 40 (2003) 955.

Husdon, J.A. (2010). Underground Radioactive Waste Disposal - The Rock Mechanics Contribution. Proceedings of the ISRM International Symposium 2010 & 6th ARMS. New Delhi. Ed. Central Board for Irrigation and Energy.

Ljunggren, C., Yanting Chang, Janson, T. & Christiansson, R. (2003). An overview of rock stress measurement methods. International Journal of Rock Mechanics & Mining Sciences 40 (2003) 975–989.

Migliazza M.R., Ferrero A.M., Spagnoli (2011) A Experimental analysis of crack propagation in Carrara marble subjected to cyclic loads. International journal of rock mechanics (ISSN:1365-1609). 1038- 1044. N 48.

Segalini A., Ferrero A.M., Giani G.P. (2009) Stability analysis of historic underground quarries Computers and Geotechnics **ISSN:** 0266-352X doi:10.1016/j.compgeo.2010.01.007

Sjöberg, J., Christiansson, R. & Hudson, J.A. (2003). ISRM Suggested Methods for rock stress estimation—Part 2: overcoring methods. International Journal of Rock Mechanics & Mining Sciences 40 (2003) 999–1010.

Su S., Stephansson O. (1999) - *"Effect of a fault on in situ stresses studied by the distinct element method"* - International Journal of Rock Mechanics and Mining Sciences 36, Elsevier Science;

Worotnicki G. (1993) - *"CSIRO triaxial stress measurement cell* - CSIRO, Mount Waverley, Australia.

"3DEC Command reference" Itasca Consulting Group, Inc. (1998), Minneapolis, Minnesota (USA);

"3DEC User's guide" Itasca Consulting Group, Inc. (1998), Minneapolis, Minnesota (USA);

Figure
Click here to download Figure: figure.docx

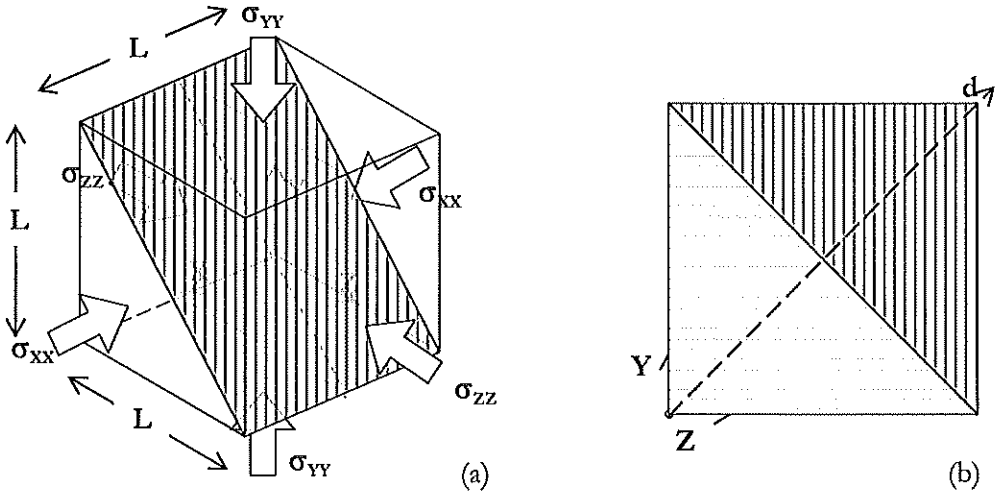

Figure 1 – Geometry of the 3D DEM model and its loading condition (a); vertical section considered for the comparison of the results (b).

Figure 2 – Main stresses in the central section parallel to the axis with a friction angle equal to 5°.

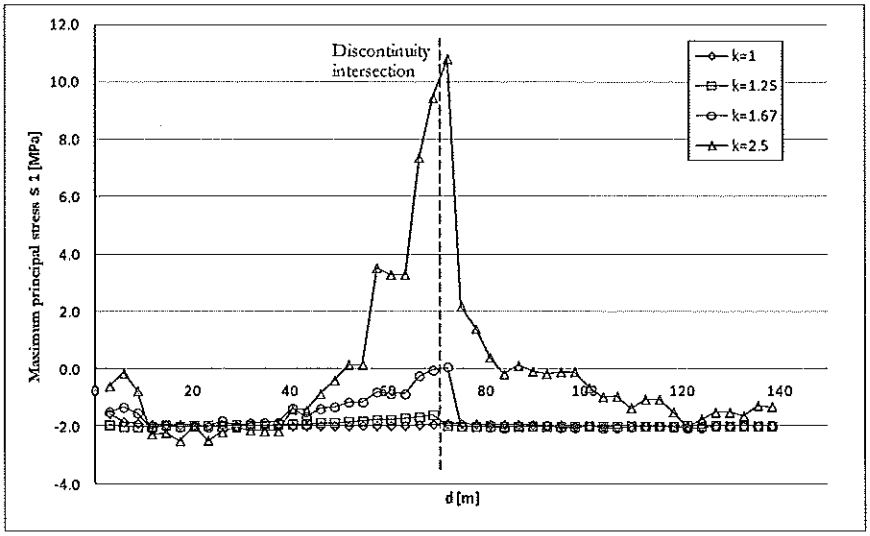

Figure 3 – Maximum main compression stresses

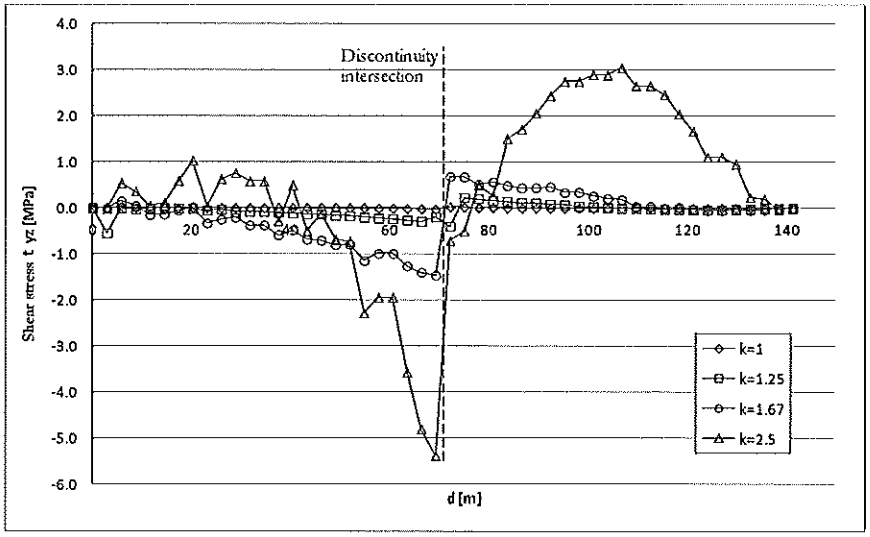

Figure 4– Shear stresses along the discontinuity

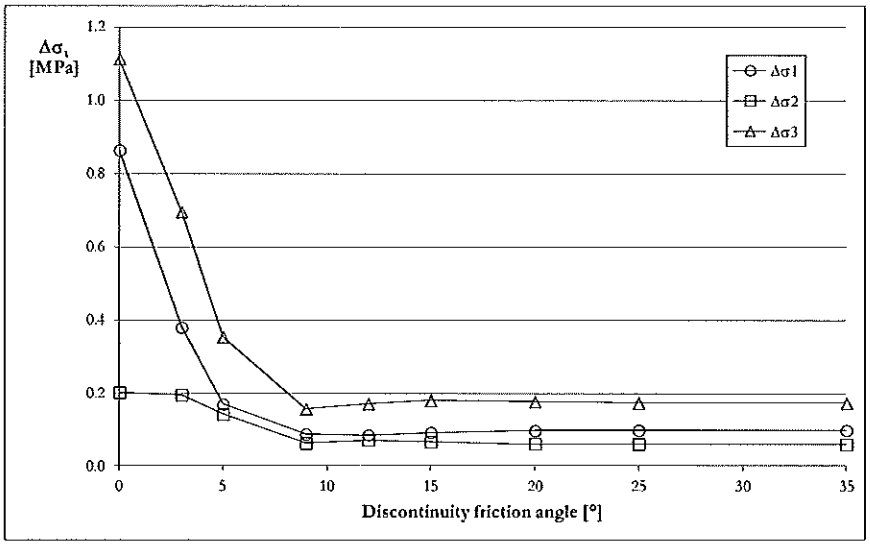

Figure 5- Differences in the main stresses in correspondence to the discontinuity in function of the friction angle – (K_o = 1.25)

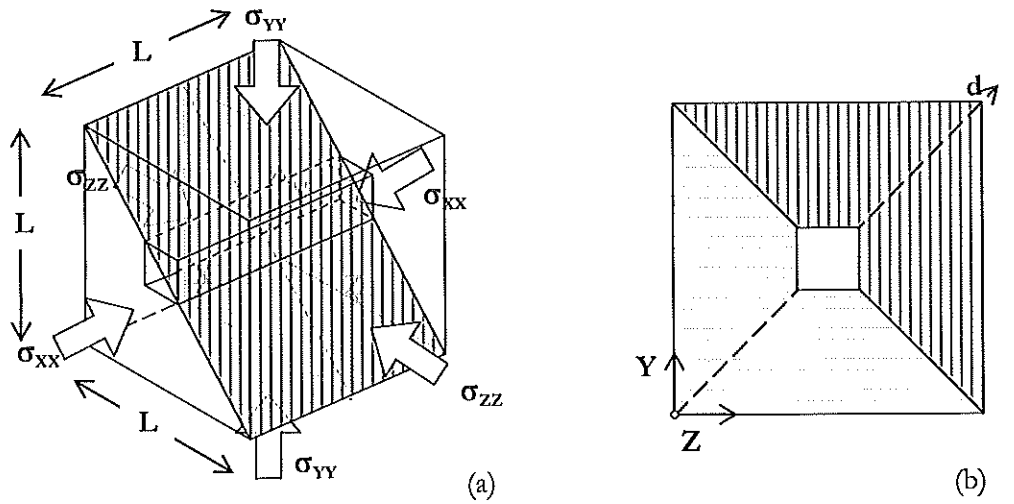

Figure 6– Configuration of the model and the reference system

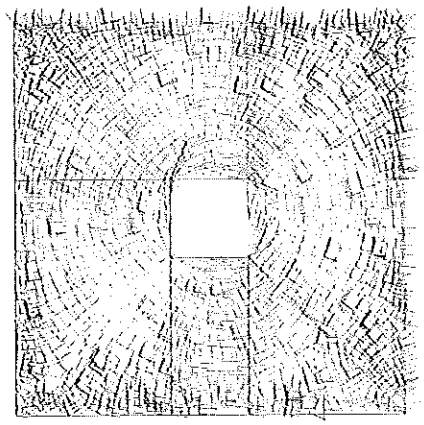

Figure 7– Main stresses in the central section parallel to the z axis

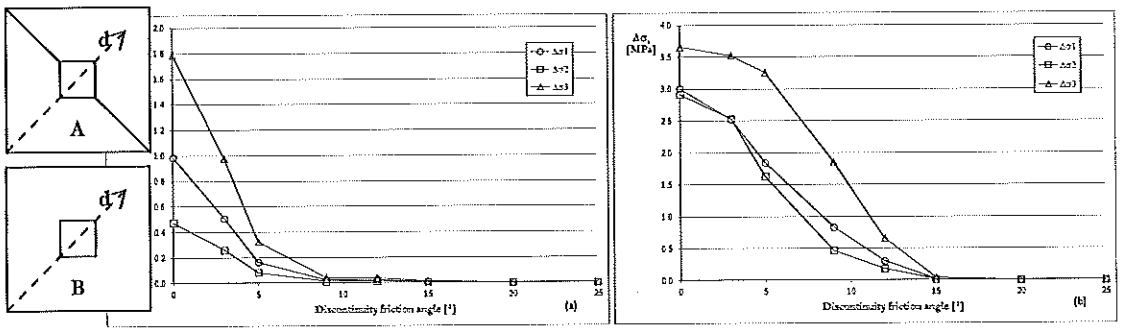

$$\Delta\sigma_i = \max\left[\Delta\sigma_{iA}(d) - \Delta\sigma_{iB}(d)\right]$$

Figure 8- Differences in the maximum main stresses in correspondence to the discontinuity in function of the friction angle F ($K_o = 1.25$)

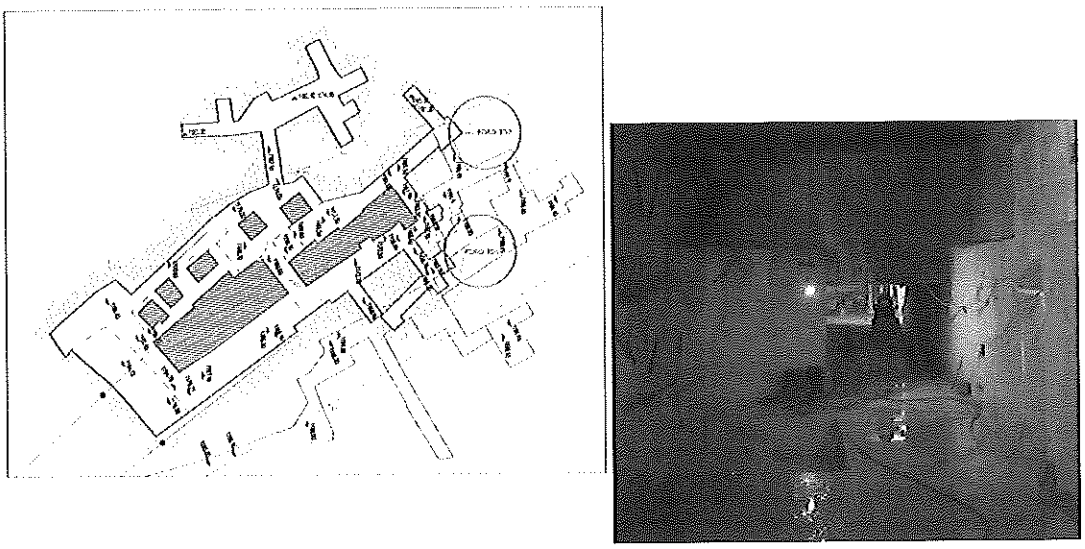

Figure 9– Quarry excavation maps with indication of the in situ stress measurement points

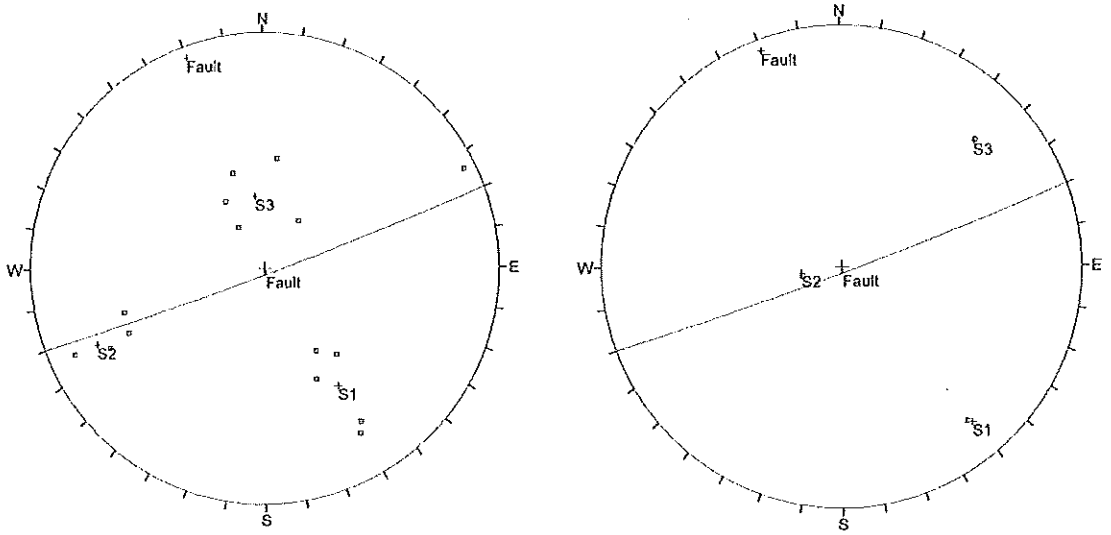

Figure 10- Representation of the network of action of the main stresses for the D1 tests (on the left) and D2 tests (on the right).

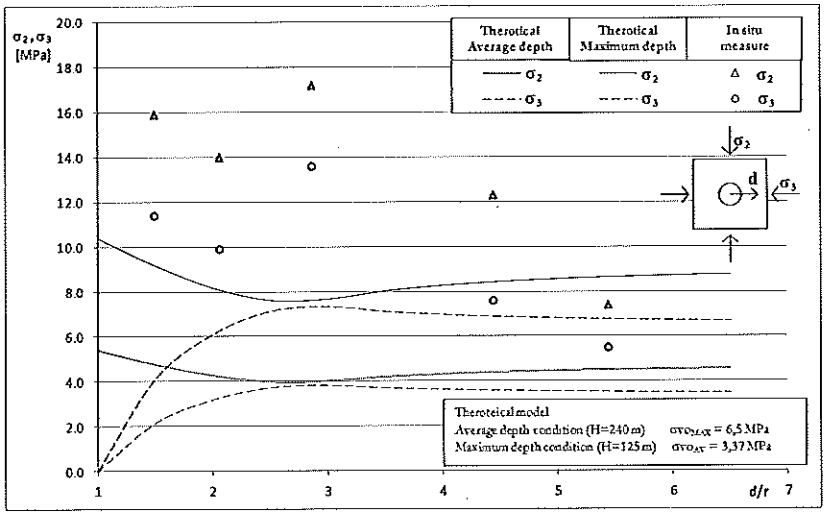

Figure 11 – Comparison between the main in situ measured stress components and theoretical values calculated in an elastic field for a circular tunnel subject to an anisotropic stress state at different depths.

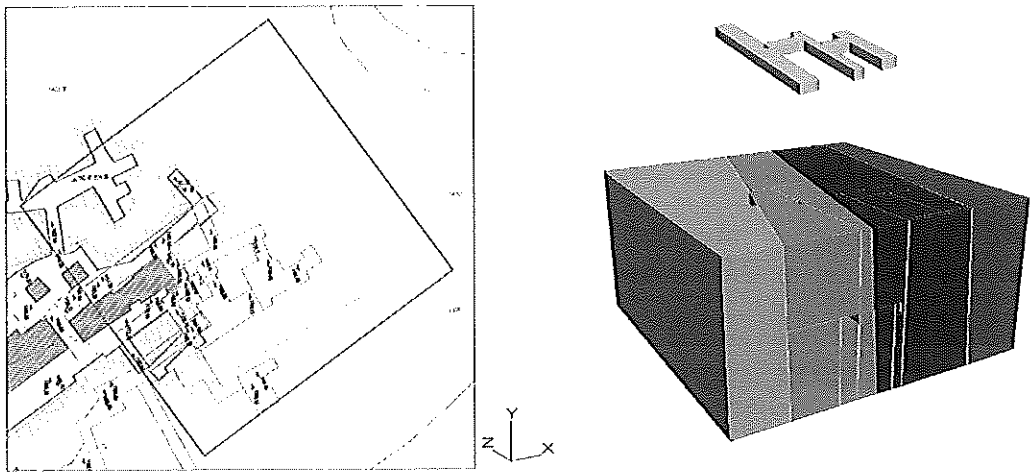

Figure 12– Analysed portion of the excavation chamber and its simplification (a); geometric model utilised (b)

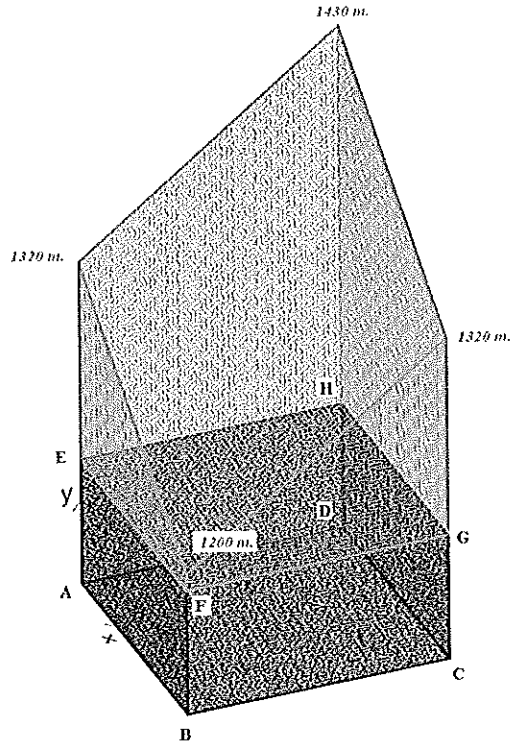

Figure 13– Geometry of the loads.

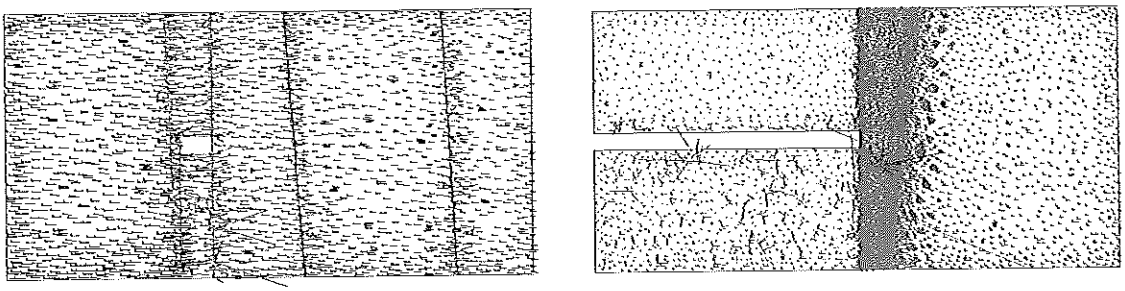

Figure 14– Transversal and longitudinal sections of the model with respect to the excavation axis and representation of the main stress components.

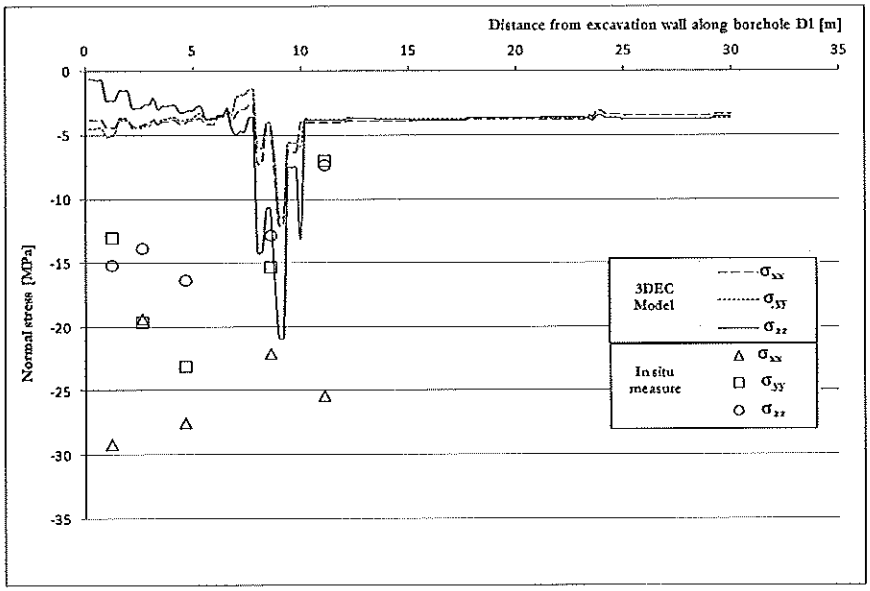

Figure 15 – Comparison of the in situ measured and D1 numerical modelling stresses.

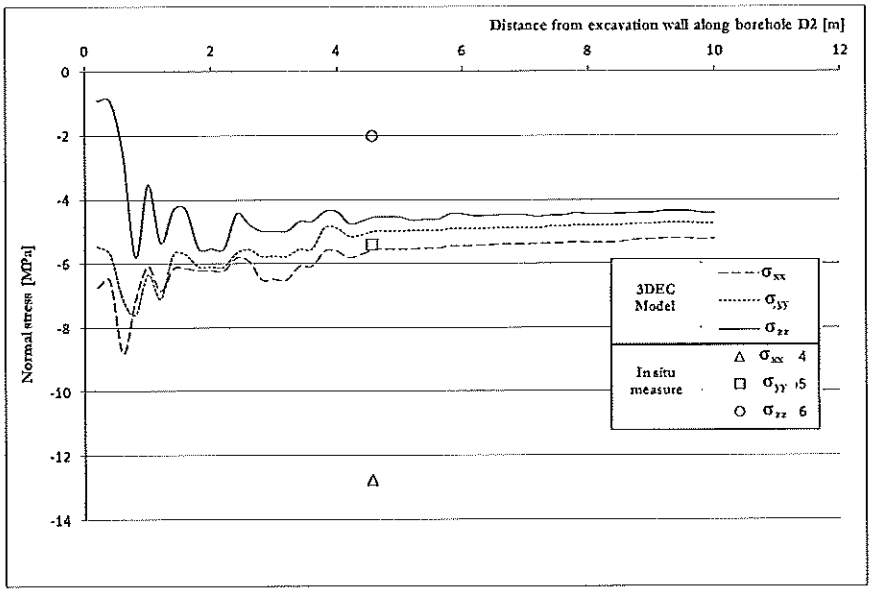

Figure 16 – Comparison of the in situ measured and D2 numerical modelling stresses.

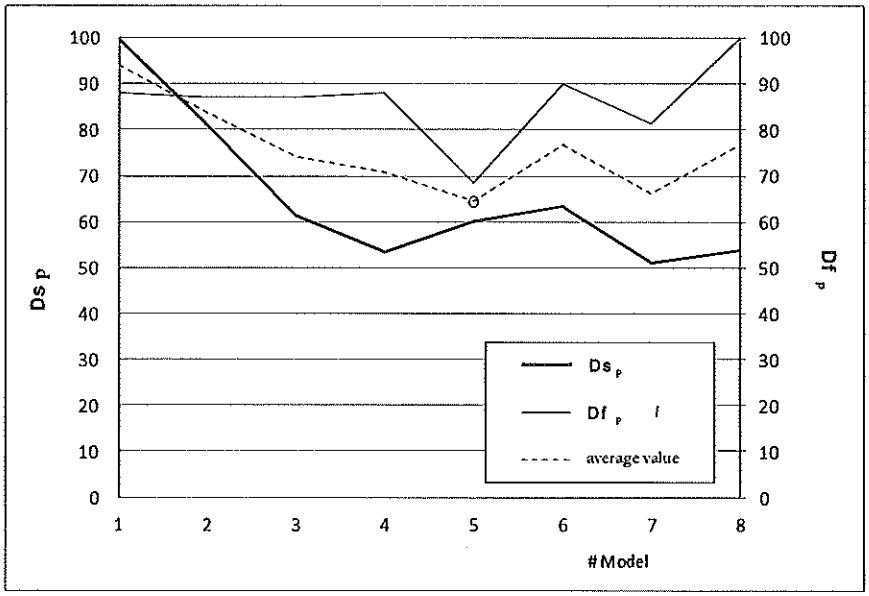

Figure 17- Equivalent percentage errors calculated for each analysed model.

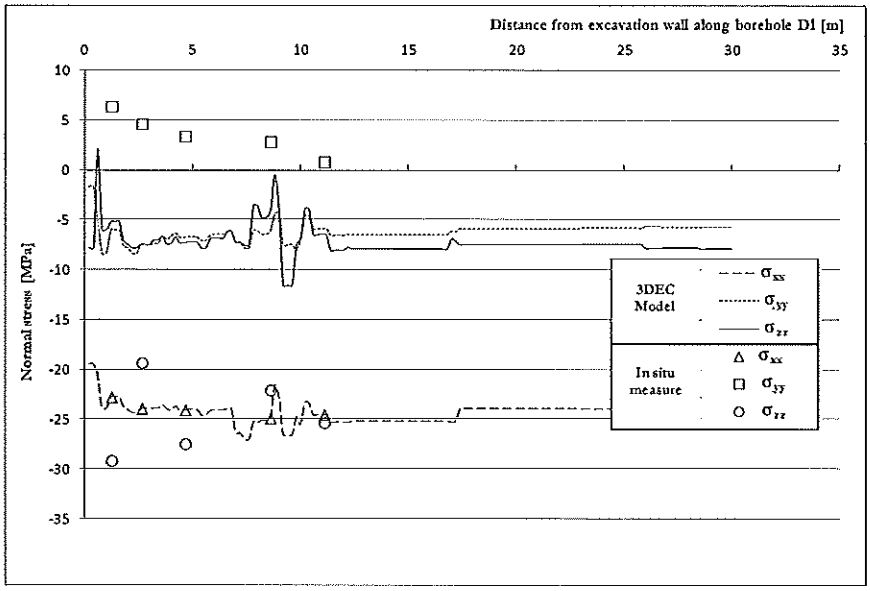

Figure 18. Comparison between the measured and computed stresses in the borehole 5